

Preparation and Insecticidal Activity Evaluation of Emamectin–Lignin Sulfonic Acid Conjugate with Antiphotolysis Property

Yanmin Huang, Xiangying Li, Qipeng Xiong, Yong Chen, Zining Peng, Jinghong Chen, Junyan Li, Yuanfei Zhang, and Jianguo Cui*



Cite This: *ACS Omega* 2022, 7, 29046–29053



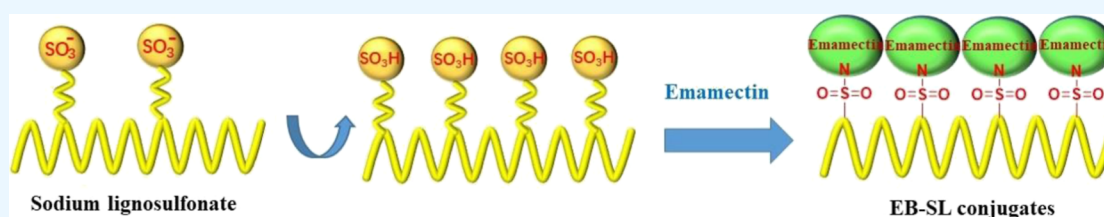
Read Online

ACCESS |

Metrics & More

Article Recommendations

Supporting Information



ABSTRACT: Controlled release formulations (CRFs) are considered an effective way to solve the low bioavailability of traditional pesticides. However, CRFs prepared by coating or encapsulation has the disadvantage of explosive release of the ingredients. Sustained-release pesticides prepared by coupling with a carrier can overcome this shortcoming. In the present study, an emamectin–lignin sulfonic acid conjugate (EB–SL), in which emamectin was connected *via* sulfonamide bonds with lignin, was prepared using sodium lignosulfonate as the carrier. The structure of the conjugate was characterized by IR, ¹HNMR, and elemental analysis. The sustained-release results showed that EB–SL maintained its original structure when released in pure water and soil columns, and the sulfamide bond did not break. The photolysis test displayed that the photolysis half-life $T_{0.5}$ of EB–SL was increased by 1.5 times compared with the emamectin suspending concentrate (EB–SC). Bioactivity tests in the greenhouse showed that EB–SL not only had similar insecticidal toxicity to emamectin emulsion concentrate (EB–EC) against *Ostrinia nubilalis* but also displayed a longer duration. The lethality of EB–SL on *O. nubilalis* was maintained at more than 70% across 19 days, whereas EB–EC as the control was less than 50% after 11 days of application.

1. INTRODUCTION

Pesticides play a crucial role in ensuring stability and high yield in agricultural production.^{1,2} However, the actual bioavailability of traditional pesticide formulations is greatly reduced due to the loss of pesticide ingredients and unexpected degradation in the environment after application. The result is the excessive use of pesticides, which not only increases agricultural production costs but also brings a negative impact on the environment safety.^{3,4} At present, controlled release formulations (CRFs) are considered an effective way to solve the above problems.⁵

CRFs refer to the release of the active ingredients of the pesticides within set conditions and time. The application of CRFs can reduce damage to the environment caused by the excessive use of pesticides, decrease the influence of pesticides on nontarget organisms and the environment, and have economic and ecological advantages. It is an important technical direction for the green development of pesticides.⁶ Preparation of CRFs is generally carried out by coating or encapsulation and adsorption or coupling of the carriers with ingredients.^{7,8} Generally, the wrapping matrix uses polymers, such as polylactic acid, polyacrylic acid, polyvinyl alcohol, and

so forth.⁹ In recent years, the use of natural polymer of lignin or polysaccharides as the matrix for CRFs has attracted more attention due to their low cost, nontoxicity, rich sources, biodegradability, environmental friend, and renewability.^{10,11}

The coating or encapsulation has the advantage of keeping the structure of the active ingredients unchanged. However, due to the weak force between the matrix and the components, explosive release of the ingredients can occur during use, making the release process difficult to control.¹² Sustained-release pesticides prepared by coupling with a carrier can overcome this shortcoming. Since the active ingredient is coupled to the carrier through a chemical bond, it is generally stable. The killing of a pest can only be achieved after the pesticide has entered its body and separated the active ingredient through the action of biological enzymes.^{13–15}

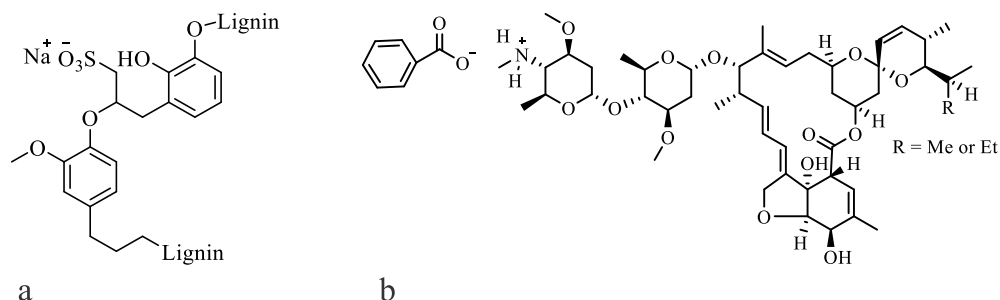
Received: May 9, 2022

Accepted: July 29, 2022

Published: August 9, 2022



Scheme 1. Structure of (a) Sodium Lignosulfonate and (b) Emamectin Benzoate



Sodium lignosulfonate is an industrial product derived from natural lignin (Scheme 1),^{16,17} which is composed mainly of molecules with a polyphenol structure and has excellent antioxidation and resistance to photolysis and biodegradability.^{18,19} Many researchers have conducted in-depth research on the utilization of lignin through chemical modification.^{20–23}

Emamectin benzoate (EB) is a macrocyclic lactone obtained by the semisynthesis of avermectin,²⁴ and has been widely used in the prevention and control of lepidopterous pests because of its high efficiency and low toxicity.²⁵ However, it is easily photodegraded due to the presence of the conjugated double bond in the structure.²⁶ Researchers have made various attempts to slow down its photodegradation, such as preparing EB sustained-release formulations by adsorption,²⁷ encapsulation,²⁸ or embedding,^{29,30} and achieved better antiphotolysis effects. Nevertheless, there have been few reports in the literature on improving the antiphotolytic stability of emamectin by means of coupling with a carrier.

In the previous study, we used sodium lignosulfonate as a carrier and utilized the charge interaction between the sulfonate anion in sodium lignosulfonate and the methylamino positive ion in emamectin to prepare an emamectin nanoformulation with a particle size of 150–200 nm and good resistance to photolysis.³¹ In the present study, sodium lignosulfonate was used as a carrier and connected to the methylamino group of emamectin through sulfonamide bonds. A novel emamectin–lignosulfonate conjugate was prepared, its structure was characterized, the release in water and soil was analyzed, and the antiphotolysis performance and insecticidal activity were further evaluated.

2. MATERIALS AND METHODS

2.1. Materials. EB was obtained from Hebei Weiyuan Bio-Chemical Co., Ltd., China (Tech. 68%); sodium lignosulfonate from Tianjin Fuchen Chemical Reagent Co. Ltd., China. (AR); DMF from Shanghai Shenbo Chemical Co., Ltd., China (AR); triethylamine (AR), thionyl chloride (AR), sodium hydroxide (AR), and ethanol (AR) were purchased from Guangdong Guanghua Sci-Tech Co., Ltd., China. The commercial EB suspension concentrate (EB-SC, 3.0%) and emamectin emulsion concentrate (EB-EC, 5.7%) were provided by Guangxi Tianyuan Biochemical Co. Ltd., China.

2.2. Methods. **2.2.1. Preparation of the Emamectin–Lignosulfonic Acid Conjugate (EB–SL).** **2.2.1.1. Preparation of Modified Lignosulfonic Acid.**³² 20 g of sodium lignosulfonate (SL) was placed in a round-bottom flask, and 50 mL of deionized water was added to dissolve it. Then, 3 mL of 30% hydrogen peroxide was slowly added to it on an ice bath and heated to 80 °C. The reaction was stirred at this temperature

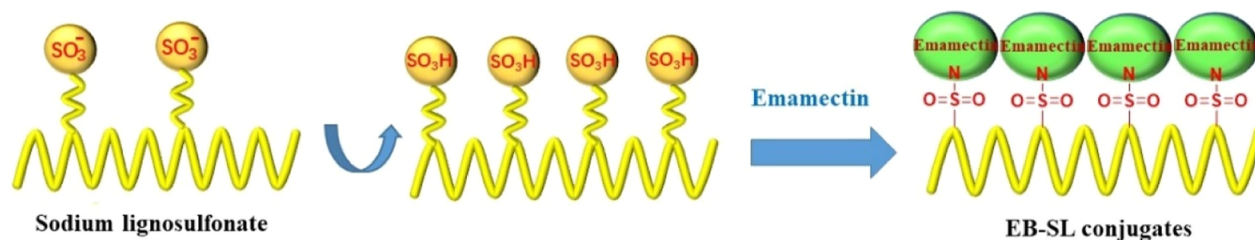
for 2 h. Then, 8 g of sodium sulfite and 2 g of formaldehyde were added, adjusting the pH to 8–10. The resulting solution was further heated to 90 °C, stirred continuously for 4 h, and then cooled to room temperature. 1 M hydrochloric acid was added dropwise to the cooled solution to precipitate lignosulfonic acid. The precipitate was washed with alcohol, filtered, and dried at 80 °C to obtain 9.6 g of brown powdery lignosulfonic acid with a yield of 48% and a reaction efficiency of 37.9%.

2.2.1.2. Preparation of EB–SL. 10 mL of anhydrous DMF was added into a three-necked round-bottom flask, and then 1 g of dried lignosulfonic acid was added and stirred to dissolve, and the temperature was lowered to 0 °C. Next, 2 mL of thionyl chloride was added to the reaction solution with a syringe and reacted for 5 h at 0 °C. Finally, lignin sulfonyl chloride was obtained. The superfluous thionyl chloride was removed from the lignin sulfonyl chloride under reduced pressure. Then, 8 mL of anhydrous triethylamine was added, adjusting the pH to 9–10. Subsequently, EB solution (1.5 g of 68% EB was dissolved in 10 mL of anhydrous dichloromethane, with a total of 1.02 g of EB) was added, and the mixture was stirred at room temperature for 5 h. After the reaction was completed, the dichloromethane was removed under reduced pressure to obtain a brown solid. It was extracted and washed with dichloromethane and saturated brine, and the solvent was removed from the organic layer under reduced pressure to obtain unreacted EB. The brown flocs floating in the water layer were filtered and further washed repeatedly with deionized water to remove DMF, and the product was dried at 60 °C to obtain 0.63 g of brown EB–SL with a yield of 47.7%. 0.70 g of EB did not participate in the reaction, while the amount of EB that participated in the reaction was 0.32 g, and the substitution rate was 31.3% (see the Supporting Information for the calculation method).³³

2.2.2. Structural Characterization of the EB–SL Conjugate. Infrared spectroscopy was determined by using a Thermo Scientific IS-10 Fourier infrared spectrometer, test conditions: 4000–400 cm⁻¹, resolution 4 cm⁻¹; the ¹H NMR spectra were recorded on a Bruker AV-600 spectrometer at working frequencies 600 MHz and scanned 32 times. Elemental analysis was done using a Vario EL Cube elemental analyzer (Germany), which heated the sample furnace to 1150 °C.

Morphology of the EB–SL conjugate was observed on a scanning electron microscope (cold-field transmission electron microscope, Hitachi SU8010, Japan) at a test voltage of 3 kV and test current of 10 μA. Sample preparation: a small piece of conductive tape was stuck on the sample table. A small amount of sample was scattered evenly on the carbon conductive tape, and then the excess unstuck powder was blown off. It was then

Scheme 2. Fabrication Mechanism of the Emamectin–Lignosulfonic Acid Conjugate (EB–SL)



placed into the gold spraying instrument for a spraying time of 10 mA—120 s. Finally, the sample was observed using an electron microscope.

2.2.3. Release Behavior of the EB–SL Conjugate.

2.2.3.1. Release of the EB–SL Conjugate in 50% Methanol–Water. The dialysis bag diffusion method was used to determine the release behavior of the EB–SL conjugate (dialysis bag, cutting $M_w = 3500$ Da). A specific quantity of samples was weighed and put into a dialysis bag, several small glass beads were added, both ends of the dialysis bag were fastened tightly, and it was placed into a 100 mL open-mouth bottle. A corresponding EB–SC was used as a control. Then, 100 mL of 50% methanol–water mixture (pH = 7) was added to the bottle, with three parallels for each sample, and placed in a shaker ($T = 25$ °C, speed 180 rpm). The first sampling was taken after 3 h and then every 12 h. After each sampling, the solution was replaced with a fresh solvent and put back in the shaker to release again. The absorbance of the solution was analyzed using an ultraviolet–visible spectrometer [Shimadzu Enterprise Management (China) Co., Ltd., model: UV-2600], and the content of emamectin was converted from the standard curve. The cumulative release rate of the sample was calculated according to [formula 1](#)

$$Q (\%) = \frac{\sum (V \times ct)}{W} \times 100\% \quad (1)$$

Q: cumulative release rate; W: total weight of emamectin in samples (mg); V: the volume of each sample taken (100 mL); ct: the concentration of emamectin per sampling (mg/mL).

2.2.3.2. Release of the EB–SL Conjugate in a Soil Column.

A plexiglass tube with an outer diameter of 40 mm, an inner diameter of 32 mm, and a column length of 25 cm was used. The lower end nozzle of the column was wrapped and sealed with gauze. The column was filled with 120 g of the soil (sampled from a sugarcane field, crushed, and passed through a 30-mesh sieve) to 15 cm height. Then, 100 mg of the sample was added to the upper part of the soil. Immediately, 1 cm thick soil was added to the top of the sample, and a piece of filter paper laid on the top. Water was added to the filter paper at the rate of 2 drops per minute, and the exudate solution was collected at predesigned times to determine the content of emamectin. All the experiments were carried out in triplicate.

2.2.4. Photostability of Emamectin in the EB–SL Conjugate. The EB–SL conjugate was diluted with deionized water to 2 mg/mL, and the same concentration of EB–SC was used as a control. Then, 1 mL per well was added to the 24-well culture plate, which was sealed with a transparent plastic film and placed under a UV lamp (40 W, wavelength: 253 nm) at a 45 cm distance. Irradiated samples were collected at predesigned time intervals, diluted in methanol, transferred to a 10 mL volumetric flask, and diluted to the scale. The resulting samples were measured with a UV–visible

spectrophotometer to record the maximum absorbance of emamectin, and the content of undecomposed emamectin was calculated according to the standard curve $Y = 42.616X + 0.238$ ($R^2 = 0.9997$).

2.2.5. Insecticidal Activity Assay of the EB–SL Conjugate.

2.2.5.1. Insecticidal Toxicity of the EB–SL Conjugate at Different Concentrations. The toxicity test was conducted on *Ostrinia nubilalis* (third instar). The samples were diluted with deionized water to different concentrations (100, 25, 6.25, 1.56, 0.39, and 0.1 ppm). Fresh corn leaves were cut into appropriate lengths and then soaked in the corresponding concentration of formulation for 10 s, using deionized water as the blank control and EB–EC as the positive control. After air-drying, corn leaves were transferred to the $11 \times 7.5 \times 4$ cm culture boxes with filter paper at the bottom. Then, 40 healthy *O. nubilalis* were gently introduced into each culture box and sealed with a plastic cover with small holes. The culture boxes were kept in a pest control room (light/darkness = 16:8, temperature = 25 ± 2 °C, relative humidity = $75 \pm 5\%$), and the lethality rate of the insects was investigated after 48 h. Four replications were carried out for comparison and calculated as follows

$$M (\text{mortality rate, } \%) = \frac{n/n_0 - n'/n_0}{100 - n'/n_0} \times 100\% \quad (2)$$

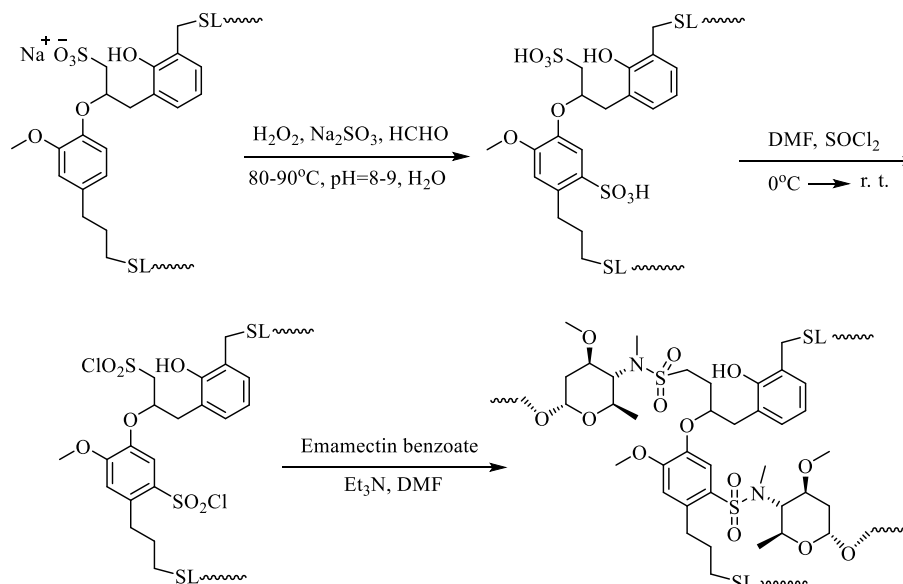
n is the number of dead insects, n' is the number of dead insects in the blank control, and n_0 is the total number of insects added to the box.

2.2.5.2. Insecticidal Duration of the EB–SL Conjugate. An appropriate amount of soil was put in a $\varphi 28 \times 20$ cm plastic pot, and then five corn seeds were planted in each pot. After the plants were grown in the greenhouse for 15 days, 100 ppm EB–SL conjugate was evenly smeared on the leaves with a brush at different time intervals (0, 3, 7, 11, 15, and 19 days), using EB–EC as the control. Three pots were used as the blank control without spraying formulation. Finally, the leaves of the corn plants were collected to determine their insecticidal activity according to the above test method. Four replications were carried out for comparison, and the insecticidal duration of the samples was determined according to the lethality rate of *O. nubilalis* at different time.

2.2.6. Assay in Vitro on Cytotoxicity of the EB–SL Conjugate. Following the test method in the ref 34, human normal kidney epithelial cells (HEK293T) were selected as the test cells.

2.2.7. Statistical Analysis. All experimental data are expressed in mean standard deviation. Significant differences between the experimental replicates were checked using one-way ANOVA and Duncan's multiple range test. $p < 0.05$ indicates statistical significance.

Scheme 3. Synthetic Route of the Emamectin–Lignosulfonic Acid Conjugate (EB–SL)



3. RESULTS AND DISCUSSION

3.1. Preparation of the EB–SL Conjugate. The preparation mechanism of EB–SL conjugate is shown in Scheme 2:

First, sodium lignosulfonate was further sulfonated to improve its sulfonation degree and increase the proportion of sulfonic acid groups in the molecule to augment the degree of substitution between lignin and emamectin. In the next reaction, thionyl chloride was used to convert the sulfonic acid group into a more active sulfonyl chloride and then reacted directly with emamectin without separation. The conjugate of emamectin with lignosulfonic acid (EB–SL) was obtained through the formation of a sulfonamide bond (Scheme 3).

3.2. Structural Characterization of the EB–SL Conjugate. **3.2.1. Infrared Spectral Analysis.** Figure 1 is the infrared spectra comparison of EB–SL, sodium lignosulfonate (SL), and EB. Among them, 1732.6 cm^{-1} is the characteristic absorption peak of the ester group of EB. Compared with EB, the characteristic absorption peak of the ester group in EB–SL has not changed. However, EB–SL increases a strong

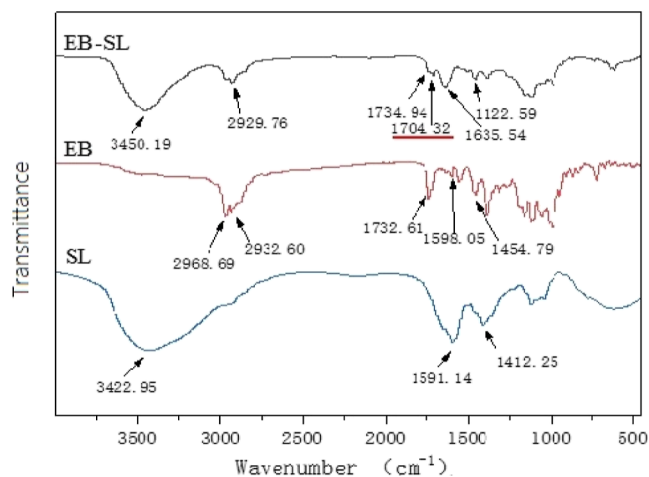


Figure 1. Infrared spectra comparison of the EB–SL conjugate, sodium lignosulfonate (SL), and EB.

absorption peak at 1635 cm^{-1} , which is the stretching vibration absorption of the newly formed sulfonamide bond. Additionally, for the EB–SL conjugate, the NH and OH absorption peak of lignin at 3450 cm^{-1} is weaker than that of the sodium lignosulfonate (SL), and the stretching vibration absorption of the alkyl group appears at about 2930 cm^{-1} , indicating that the emamectin has connected with lignin *via* the sulfonamide bond.

3.2.2. ^1H NMR Analysis of EB–SL. Figure 2 shows the ^1H NMR comparison of EB–SL and EB. When emamectin was bonded with lignosulfonic acid, the hydrogen on the methylamino group in the emamectin was substituted to form a sulfonamide bond. At this point, the chemical shift of the methyl group on the nitrogen should be transferred from the high field to the low field. As can be seen from Figure 2, the chemical shift of the methyl group connected to nitrogen had shifted from 2.57 ppm in the high field to 2.81 ppm in the low field, indicating that the sulfonamide bond had been formed and the emamectin had been coupled with lignosulfonate.

3.2.3. Elemental Analysis. As shown in Table 1, compared with the original SL, the content of S and O elements in modified SL is significantly increased, indicating that SL had been further sulfonated, and more sulfonate groups were introduced into lignin. Compared with modified SL, the content of N and C in EB–SL is significantly increased, while the content of O is reduced, indicating that EB has been successfully combined with lignosulfonate.

3.3. Microtopography Characterization of the EB–SL Conjugate. Figure 3 shows SEM images of EB–SL, with SL used as the comparison. As shown in Figure 3, the appearance of SL is a loose and soft structure, but after it forms the conjugate with emamectin, a compact structure is yielded. It shows that after combining with emamectin, the surface structure of sodium lignosulfonate has also been changed due to the change in the chemical structure.

3.4. Release Analysis of the EB–SL Conjugate under Different Conditions. **3.4.1. Release of the EB–SL Conjugate in 50% Methanol–Water.** Figure 4 shows the release behavior of EB–SL in 50% methanol–water. As shown in the figure, the release of EB–SC as a control was completed

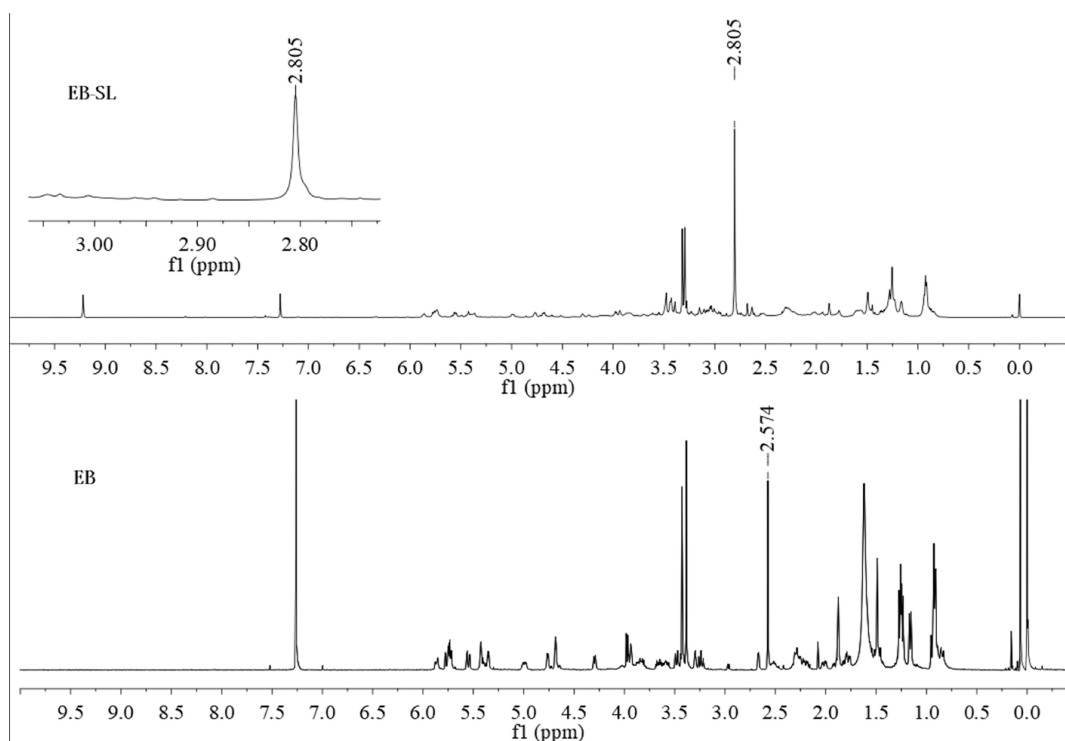
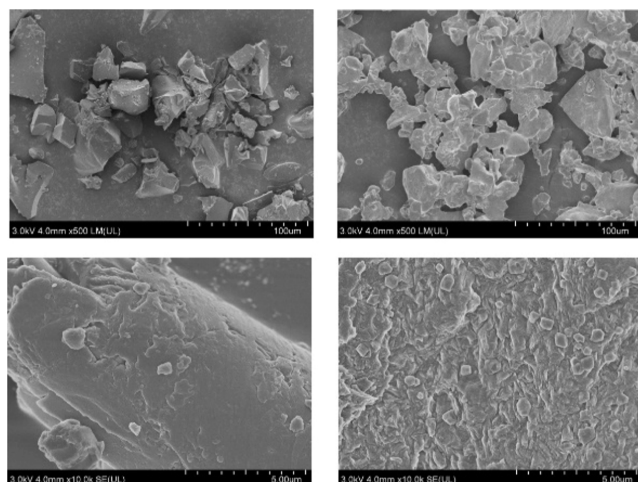


Figure 2. ^1H NMR comparison of the EB–SL conjugate and emamectin (EB).

Table 1. Results of Elemental Analysis for SL and EB–SL

name	N %	C %	H %	S %	O %
SL	0.400	33.22	4.274	1.417	12.232
modified SL	0.580	29.14	3.595	6.615	40.788
EB–SL	3.090	55.55	7.383	6.722	22.093



EB-SL

SL

Figure 3. Scanning electron microscopy of the EB–SL conjugate and sodium lignosulfonate (SL).

at 93 h, but EB–SL released about 15% in the first 3 h and did not release in the later period. The sulfonamide bond in EB–SL cannot be broken in 50% methanol–water to release emamectin. The emamectin released in the first 3 h is the free emamectin without bonding.

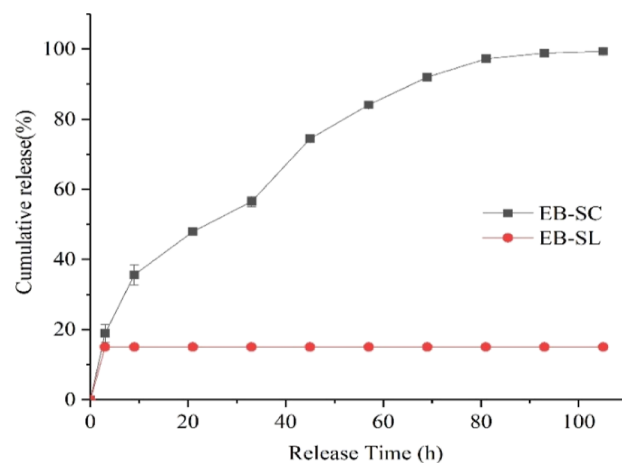


Figure 4. Release curve of the EB–SL conjugate and EB-SC in 50% methanol–water (25 °C).

3.4.2. Release of the EB–SL Conjugate in Soil. Figure 5 is a release diagram of EB–SL in soil. As can be seen, 95% of EB–SC was released by the fourth day, and all of it was released by the sixth day, while EB–SL released 40% by the fourth day and was completely released on the 14th day.

However, by analyzing the UV–vis absorption spectra of EB–SC and EB–SL leachate, it was found that the release of EB–SL in the soil is a simple process of dissolution and dialysis without breaking the sulfonamide bond. The UV–vis spectra of both were consistent before and after the release of EB–SL in the soil column. Compared with EB–SC, there was an obvious lignin absorption peak at 275 nm in EB–SL (Figure 6).

3.5. Antiphotolysis Assay of the EB–SL Conjugate. Figure 7 is a comparison diagram of the resistance to photolysis of EB–SL and EB–SC. The photolysis rate of EB

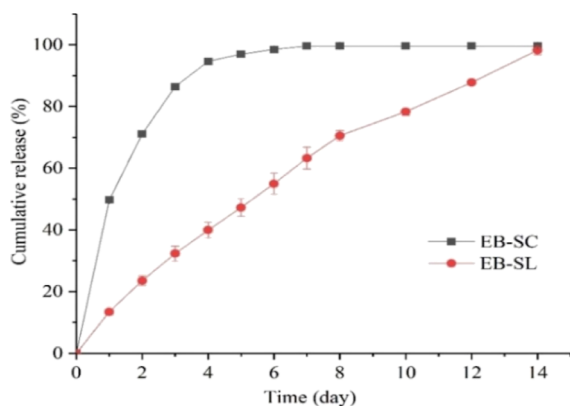


Figure 5. Release curve of the EB-SL conjugate and EB-SC in soil.

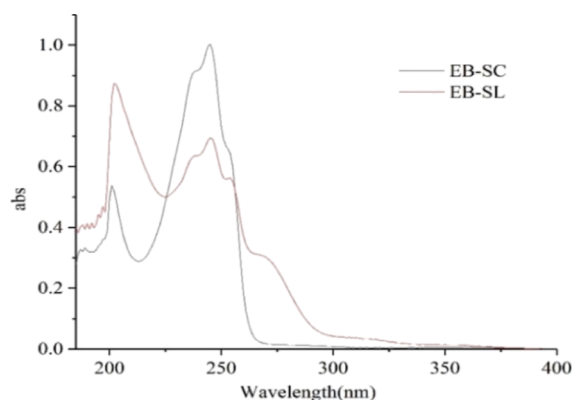


Figure 6. UV-vis spectra of leachate of EB-SL and EB-SC.

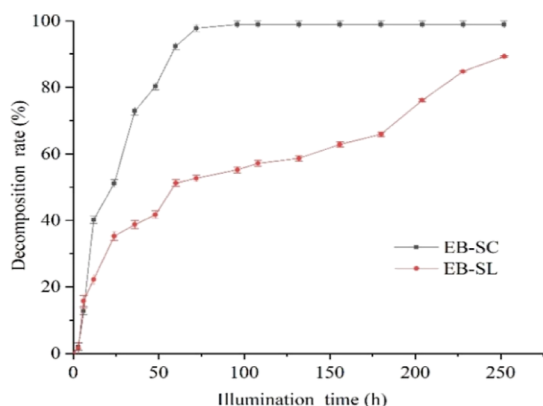


Figure 7. Comparison of photolysis curves of the EB-SL conjugate and EB-SC.

in EB-SC reached 51% at 24 h, and the photolysis was basically completed at 96 h. The photolysis rate of EB-SL was 51% at 60 h and 85% after 252 h. From the curve in the figure, the photolysis rate of EB-SL is faster in the first 60 h and slower in the second half. The photolysis half-life $T_{0.5}$ of EB-SL is 1.5 times longer than that of EB-SC. This is because SL absorbs a large amount of ultraviolet light in the illumination process, thus greatly improving the stability of EB.

3.6. Insecticidal Activity of the EB-SL Conjugate.

3.6.1. Insecticidal Toxicity at Different Concentrations. An insecticidal toxicity test was performed on EB-SL, and commercial EB-EC was used as the control. Figure 8 shows the lethality of EB-SL at different concentrations against *O.*

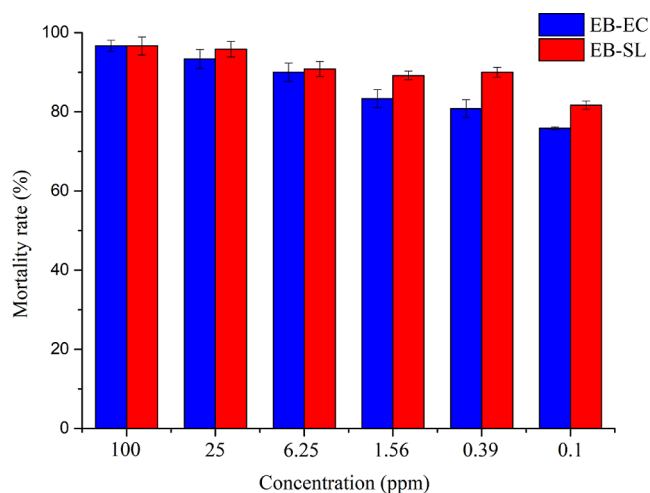


Figure 8. Insecticidal toxicity comparison of the EB-SL conjugate with EB-EC at different concentrations against *O. nubilalis*.

nubilalis (mid-to-late third instars) for 48 h. The results showed that, compared with EB-EC, EB-SL did not lose the insecticidal activity of the original EB, and there was no significant difference in the insecticidal toxicity between them. The mechanism of action needs further study to ascertain how EB-SL breaks the sulfonamide bond in the organism to achieve the effect of killing pests.

3.6.2. Insecticidal Duration of the EB-SL Conjugate.

Figure 9 shows the lethality of EB-SL against *O. nubilalis* at

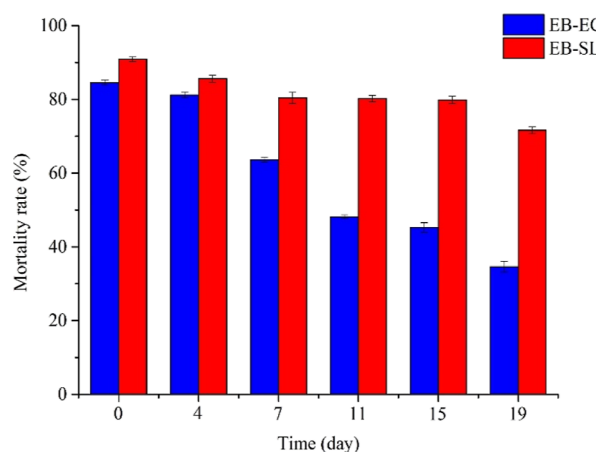


Figure 9. Insecticidal duration comparison of the EB-SL conjugate and EB-EC against *O. nubilalis* (concentration: 100 ppm).

19 day application period at a concentration of 100 ppm and EB-EC as control. The results showed that compared with EB-EC, EB-SL could maintain more than 70% insecticidal rate for 19 days, while EB-EC was less than 50% after 11 days of application. The insecticidal duration of EB-SL is significantly longer than that of EB-EC. This is primarily because after the emamectin is coupled with lignin, the lignin acts as an antiphoto-decomposition barrier, which greatly reduces the photo-decomposition of emamectin and increases its insecticidal duration.

3.7. Cytotoxic Effects of the EB-SL Conjugate.

In order to explore the cytotoxicity of EB in the human body after forming the conjugate, we determined the cytotoxicity of the EB-SL conjugate against HEK293T taking tech. EB as the

control (Figure 10). The results showed that the inhibition ratio of EB–SL against HEK293T was lower than that of tech.

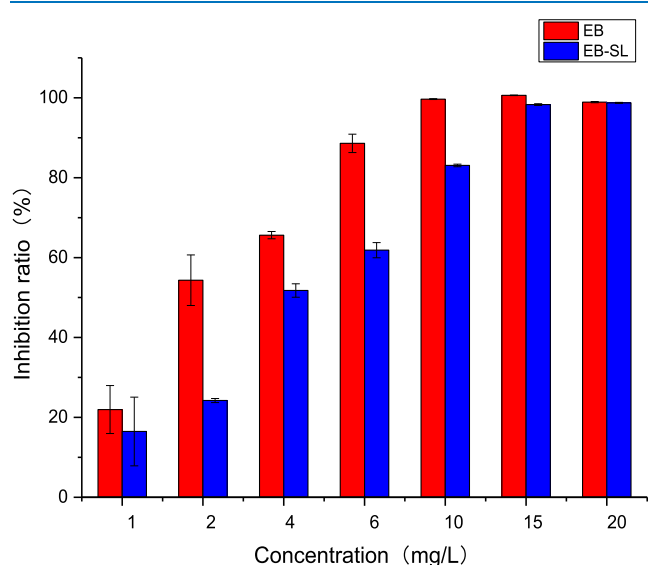


Figure 10. *In vitro* inhibition ratio of EB–SL and EB on HEK293T cells.

EB. At 6 ppm, the inhibition rate of EB against HEK-293T was 90%, while that of EB–SL was 61%. The results suggest that the cytotoxicity of EB toward the human body will be reduced after coupling with lignin to form the conjugate.

4. CONCLUSIONS

Using SL as a carrier, EB–SL, in which emamectin and lignin were connected *via* a sulfonamide bond, was successfully prepared. The release test in 50% methanol–water and a soil column showed that the conjugate maintained its original structure during the release process, and the sulfonamide bond did not break. The antiphotolysis test showed that the photolysis half-life $T_{0.5}$ of EB–SL was increased by 1.5 times compared with EB-SC. The insecticidal duration test manifested that the insecticidal lethality of the conjugate remained above 70% within 19 days, while using EB-EC as the control, it was less than 50% after 11 days of application. Meanwhile, after the emamectin was coupled with lignin, the cytotoxicity of emamectin was further reduced. Therefore, EB–SL can be used as a green insecticide for agricultural pest control in the field.

■ ASSOCIATED CONTENT

SI Supporting Information

The Supporting Information is available free of charge at <https://pubs.acs.org/doi/10.1021/acsomega.2c02883>.

Determination method of the substitution degree and reaction efficiency of modified lignosulfonic acid; cumulative release of EB–SL and EB-SC in 50% methanol–water; cumulative release of EB–SL and EB-SC in soil; photolysis stability comparison of EB–SL and EB-SC; insecticidal toxicity comparison of EB–SL and EB-EC at different concentrations against *O. nubilalis*; insecticidal duration comparison of EB–SL and EB-EC against *O. nubilalis*; and *in vitro* inhibition ratio of EB–SL and EB on HEK293T cells (PDF)

■ AUTHOR INFORMATION

Corresponding Author

Jianguo Cui – Guangxi Key Laboratory of Natural Polymer Chemistry and Physics, Nanning Normal University, Nanning 530001, PR China; Guangxi Tianyuan Biochemical Company Limited, Nanning 530001, PR China; orcid.org/0000-0002-1308-6726; Email: cuijg1954@126.com

Authors

Yanmin Huang – Guangxi Key Laboratory of Natural Polymer Chemistry and Physics, Nanning Normal University, Nanning 530001, PR China
 Xiangying Li – Guangxi Key Laboratory of Natural Polymer Chemistry and Physics, Nanning Normal University, Nanning 530001, PR China
 Qipeng Xiong – Guangxi Key Laboratory of Natural Polymer Chemistry and Physics, Nanning Normal University, Nanning 530001, PR China
 Yong Chen – Guangxi Key Laboratory of Natural Polymer Chemistry and Physics, Nanning Normal University, Nanning 530001, PR China
 Zining Peng – Guangxi Key Laboratory of Natural Polymer Chemistry and Physics, Nanning Normal University, Nanning 530001, PR China
 Jinghong Chen – Guangxi Tianyuan Biochemical Company Limited, Nanning 530001, PR China
 Junyan Li – Guangxi Key Laboratory of Natural Polymer Chemistry and Physics, Nanning Normal University, Nanning 530001, PR China
 Yuanfei Zhang – Guangxi Key Laboratory of Natural Polymer Chemistry and Physics, Nanning Normal University, Nanning 530001, PR China; orcid.org/0000-0003-2667-7055

Complete contact information is available at:

<https://pubs.acs.org/10.1021/acsomega.2c02883>

Author Contributions

J. Cui designed the project, supervised the experiments and prepared the manuscript. Y.H. supervised the experiments, collected data, and did data analysis; X.L. and Q.X. carried out the experimental work and collected data; Z.P. and J. Chen participated in some biological tests; J.L. and Y.Z. provided useful suggestions. All authors have read and agreed to the published version of the manuscript.

Funding

This work was supported by the Special Fund for Innovation-Drive Development in Guangxi of China (Major Science and Technology Project, no. AA18242027), the Guangxi Key Research and Development Program (no. AB21220015), the High-Level Innovation Team, the Distinguished Scholar Program in Guangxi colleges and universities, and the Guangxi Bagui Scholar, PR China.

Notes

The authors declare no competing financial interest.

■ REFERENCES

- Godfray, H. C. J.; Garnett, T. Food security and sustainable intensification. *Philos. Trans. R. Soc., B* **2014**, *369*, 20120273.
- McClung, C. R. Making hunger yield. *Science* **2014**, *344*, 699.
- Damalas, C. A.; Eleftherohorinos, I. G. Pesticide exposure, safety issues, and risk assessment indicators. *Int. J. Environ. Res. Public Health* **2011**, *8*, 1402.

- (4) Tilman, D.; Cassman, K. G.; Matson, P. A.; Naylor, R.; Polasky, S. Agricultural sustainability and intensive production practices. *Nature* **2002**, *418*, 671.
- (5) Chevillard, A.; Angellier-Coussy, H.; Guillard, V.; Gontard, N.; Gastaldi, E. Controlling pesticide release via structuring agropolymer and nanoclays based materials. *J. Hazard. Mater.* **2012**, *205*, 32.
- (6) Campos, E. V. R.; Oliveira, J. L.; Fraceto, L. F. Applications of controlled release systems for fungicides, herbicides, acaricides, nutrients, and plant growth hormones: a review. *Adv. Sci. Eng. Med.* **2014**, *6*, 373.
- (7) Campos, E. V. R.; de Oliveira, J. L.; Fraceto, L. F.; Singh, B. Polysaccharides as safer release systems for agrochemicals. *Agron. Sustainable Dev.* **2014**, *35*, 47.
- (8) Vemmer, M.; Patel, A. V. Review of encapsulation methods suitable for microbial biological control agents. *Biol. Control* **2013**, *67*, 380.
- (9) Babu, R. P.; O'Connor, K.; Seeram, R. Current progress on bio-based polymers and their future trends. *Prog. Biomater.* **2013**, *2*, 8.
- (10) Ismail, H.; Irani, M.; Ahmad, Z. Starch-based hydrogels: present status and applications. *Int. J. Polym. Mater. Polym. Biomater.* **2013**, *62*, 411.
- (11) Yusoff, S. N. M.; Kamari, A.; Aljafree, N. F. A. A review of materials used as carrier agents in pesticide Formulations. *Int. J. Environ. Sci. Technol.* **2016**, *13*, 2977.
- (12) Fernández-Pérez, M.; Garrido-Herrera, F. J.; González-Pradas, E.; Villafraña-Sánchez, M.; Flores-Céspedes, F. Lignin and ethyl cellulose as polymers in controlled release formulations of urea. *J. Appl. Polym. Sci.* **2008**, *108*, 3796.
- (13) Zhu, H. X.; Shen, Y.; Cui, J. X.; wang, A. Q.; Li, N. J.; Wang, C.; Cui, B.; Sun, C. J.; Zhao, X.; Wang, C. X.; et al. Avermectin loaded carboxymethyl cellulose nanoparticles with stimuli responsive and controlled release properties. *Ind. Crops Prod.* **2020**, *152*, 112497.
- (14) Ao, M. M.; Zhu, Y. C.; He, S.; Li, D. G.; Li, P. L.; Li, J. Q.; Cao, Y. Preparation and characterization of 1-naphthylacetic acid–silica conjugated nanospheres for enhancement of controlled-release performance. *Nanotechnology* **2013**, *24*, 035601.
- (15) Liu, Y.; Sun, Y.; Ding, G. L.; Geng, Q. Q.; Zhu, J. L.; Guo, M. C.; Duan, Y. H.; Wang, B. T.; Cao, Y. S. Synthesis, characterization, and application of microbe-triggered controlled-release kasugamycin–pectin conjugate. *J. Agric. Food Chem.* **2015**, *63*, 4263.
- (16) Hatakeyama, H.; Hatakeyama, T. Lignin structure, properties, and applications. *Adv. Polym. Sci.* **2009**, *232*, 1.
- (17) Li, X. N.; Qiu, X. Q.; Lou, H. M.; Ouyang, X. P.; Pang, Y. X. Influence of relative molecular mass and sulfonation degree on performance of sodium lignosulfonate as pesticide dispersant. *Fine Chem.* **2009**, *26*, 755.
- (18) Yusoff, S. N. M.; Kamari, A.; Aljafree, N. F. A. A review of materials used as carrier agents in pesticide formulations. *Int. J. Environ. Sci. Technol.* **2016**, *13*, 2977.
- (19) Richter, A. P.; Bharti, B.; Armstrong, H. B.; Brown, J. S.; Plemmons, D.; Paunov, V. N.; Stoyanov, S. D.; Velev, O. D. Synthesis and characterization of biodegradable lignin nanoparticles with tunable surface properties. *Langmuir* **2016**, *32*, 6468.
- (20) Li, Y.; Yang, D.; Lu, S.; Lao, S.; Qiu, X. Modified lignin with anionic surfactant and its application in controlled release of avermectin. *J. Agric. Food Chem.* **2018**, *66*, 3457.
- (21) Ago, M.; Tardy, B. L.; Wang, L.; Guo, J.; Khakalo, A.; Rojas, O. J. Supramolecular assemblies of lignin into nano-and microparticles. *MRS Bull.* **2017**, *42*, 371.
- (22) Pourmoazzen, Z.; Sadeghifar, H.; Yang, G. H.; Lucia, L. C. Cholesterol-modified lignin: A new avenue for green nanoparticles, meltable materials, and drug delivery. *Colloids Surf., B* **2020**, *186*, 110685.
- (23) Zhao, J. Y.; Zheng, D.; Tao, Y. H.; Li, Y. C.; Wang, L. Y.; Liu, J.; He, J.; Lei, J. D. Self-assembled pH-responsive polymeric nanoparticles based on lignin/histidine conjugate with small particle size for efficient delivery of antitumor drugs. *Biochem. Eng. J.* **2020**, *156*, 107526.
- (24) Pang, Y.; Li, X.; Wang, S.; Yang, X. D.; Lou, H. Lignin-polyurea microcapsules with anti-photolysis and sustained-release performances synthesized via pickering emulsion template. *React. Funct. Polym.* **2018**, *123*, 115.
- (25) Fengbo, F. B. Outline of the studies on emamectin benzoate. *J. Pestic. Sci. Adm.* **2002**, *3*, 003103.
- (26) Crouch, L. S.; Feely, W. F.; Arison, B. H.; VandenHeuvel, W. J.; Colwell, L. F.; Stearns, R. A.; Kline, W. F.; Wislocki, P. G. Photodegradation of avermectin B1a thin films on glass. *J. Agric. Food Chem.* **1991**, *39*, 1310.
- (27) Wang, A.; Wang, Y.; Sun, C.; Wang, C.; Cui, B.; Zhao, X.; Zeng, Z.; Yao, J.; Yang, D.; Liu, G.; Cui, H. Fabrication, characterization, and biological activity of avermectin nano-delivery systems with different particle sizes. *Nanoscale Res. Lett.* **2018**, *13*, 2.
- (28) Huang, A.; Li, X.; Liang, X.; Zhang, Y.; Hu, H.; Yin, Y.; Huang, Z. Solid-phase synthesis of cellulose acetate butyrate as microsphere wall materials for sustained release of emamectin benzoate. *Polymers* **2018**, *10*, 1381.
- (29) Elabasy, A.; Shoaib, A.; Waqas, M.; Jiang, M.; Shi, Z. Synthesis, characterization, and pesticidal activity of emamectin benzoate nanoformulations against phenacoccus solenopsis tinsley (Hemiptera: Pseudococcidae). *Molecules* **2019**, *24*, 2801.
- (30) Shoaib, A.; Waqas, M.; Elabasy, A.; Cheng, X.; Zhang, Q.; Shi, Z. Preparation and characterization of emamectin benzoate nanoformulations based on colloidal delivery systems and use in controlling *Plutellaxylostella* (L) (Lepidoptera: Plutellidae). *RSC Adv.* **2018**, *8*, 15687.
- (31) Cui, J. G.; Mo, D. M.; Jiang, Y.; Gan, C. F.; Li, W. G.; Wu, A.; Li, X. Y.; Xiao, J. A.; Hu, Q.; Yuan, H. Y.; Lu, R.; Huang, Y. M. Fabrication, characterization, and insecticidal activity evaluation of emamectin benzoate-sodium lignosulfonate nanoformulation with pH-responsive. *Ind. Eng. Chem. Res.* **2019**, *58*, 19741.
- (32) Jia, Y. J.; Sun, K.; Chen, C. Synthesis and electrochemical performance of polyaniline doped with sulfonation modified lignosulfonate. *J. Power Sources* **2018**, *42*, 1204.
- (33) Rudolph, S. E.; Glowaky, R. C. Preparation and properties of carboxyl-functional mixed esters of hydrolyzed starch. *J. Polym. Sci., Polym. Chem. Ed.* **1978**, *16*, 2129.
- (34) Huang, Y. M.; Peng, Z. N.; Wei, M. Z.; Gan, C. F.; Zhang, Y. F.; Chen, S. J.; Xiao, J. A.; Cui, J. G. Synthesis and antiproliferative evaluation of some novel estradiol selenocyanates. *Steroids* **2022**, *181*, 108992.